Green Chemistry

PAPER

Cite this: *Green Chem.*, 2020, **22**, 1605

Maleic acid as a dicarboxylic acid hydrotrope for sustainable fractionation of wood at atmospheric pressure and ≤100 °C: mode and utility of lignin esterification†

Cheng Cai,[a,b] Kolby Hirth,[b] Rolland Gleisner,[b] Hongming Lou,[a] Xueqing Qiu[a] and J. Y. Zhu *[b]

Received 13th December 2019,
Accepted 28th January 2020

DOI: 10.1039/c9gc04267a

rsc.li/greenchem

This study evaluated maleic acid (MA) as a green hydrotrope for efficient wood fractionation at atmospheric pressure and ≤100 °C. MA hydrotropic fractionation (MAHF) resulted in esterified lignin with a low degree of condensation and a very light color. 2D $^{1}H-^{13}C$ HSQC and HMBC NMR analyses of reaction products of a lignin model compound guaiacylglycerol-beta-guaiacyl ether with MA identified bonding through the γ-OH group. The surface charge of lignocellulosic MAHF water insoluble solids (WIS), induced by lignin esterification (carboxylation), enhanced enzymatic sugar yield by reducing nonproductive cellulase binding to lignin through pH-mediated electrostatic repulsion and also enhanced the lubrication effect of lignin in mechanical nanofibrillation for producing cellulose nanofibrils from WIS. Preliminary studies indicated that disssolved xylan can be dehydrated into furfural by MA in the fractionated liquor at a good yield of 70% and MA can be reused for repeated fractionation with minimal loss of less than 5%.

Introduction

Producing green energy and materials using renewable plant biomass can achieve a more sustainable future through carbon sequestration and reduced use of fossil hydrocarbons.[1] Woody biomass has the advantages of flexible harvesting time which reduces storage cost and high density that facilitates logistics and transportation. However, woody biomass is more tightly structured with a higher lignin content than herbaceous biomass, which makes lignin valorization more difficult[2] and poses a challenge for full utilization of the primary lignocellulosic components: cellulose, hemicelluloses and lignin. Conventional thermochemical fractionation methods, such as dilute acid,[3,4] steam explosion,[5] alkaline,[4] organosolv,[6–8] sulfite,[9] and commercial wood pulping processes, are all conducted at high temperatures resulting in substantial lignin condensation,[10,11] in addition to having high capital cost due to high pressure and the need for corrosion-resistant vessels. Lignin condensation poses significant difficulties for valorization, both for depolymerization to aromatics and for use as a polymeric material.[12,13] Despite recent advances made using reductive catalytic lignin fractionation,[14,15] lignin stabilization,[16] organic solvents[7,17–20] and ionic liquid systems,[21] valorization of plant biomass remains a challenge. Viable strategies will require valorization of all major components of biomass, as well as environmentally friendly and less energy intensive processes.

Acid hydrotropic fractionation (AHF) for fractionation of plant biomass has shown favorable advantages of low operating temperature at atmospheric pressure with lower-cost equipment, easy lignin separation from the fractionation liquor and hydrotrope recycling.[22,23] Using *p*-toluenesulfonic acid (*p*-TsOH) as the hydrotrope, we demonstrated that AHF has a very high selectivity at 80 °C for dissolving lignin and hemicelluloses while preserving cellulose for producing valuble materials.[22,24,25] Importantly, the dissolved lignin had a low degree of condensation primarily due to the rapid lignin dissolution.[23,26] After lignin separation, the remaining dissolved hemicelluloses can be dehydrated into furfural using *p*-TsOH in the fractionation liquor without an additional catalyst[27] and then the hydrotrope can be reused.[22] Lignin separation was accomplished through simple precipitation by diluting the fractionation liquor with water to just below the minimal hydrotrope concentration (MHC).[22,28] Because *p*-TsOH has a fairly low MHC of 11.5 wt%, diluting to the MHC requires a large amount of water. Though the dilution water can be reclaimed and reused, it is a concern for increasing the

[a]*School of Chemistry and Chemical Engineering, South China University of Technology, Guangzhou, China*
[b]*USDA Forest Service, Forest Products Lab., Madison, Wisconsin, USA. E-mail: junyong.zhu@usda.gov; Tel: +1 (608) 231-9520*

†Electronic supplementary information (ESI) available. See DOI: 10.1039/c9gc04267a

load of water evaporation for *p*-TsOH recovery and reuse. Moreover, a more mild acid would be favorable for process runnability so as to avoid potential equipment corrossion during distillation and to further reduce capital cost. The attractive advantages of low temperature, simplicity and one chemical separation for all three major components of plant biomass compelled us to seek alternative acid hydrotropes for lignin separation for better hydrotrope recycling, reduced capital cost and lower environmental impact.

Some long-chain dicarboxylic acids, such as commercial DIACID C_{21} (5-carboxy-4-hexyl-2-cyclohexene-1-yl octanoic acid), have hydrotropic properties.[29–31] However, to our knowledge this class of compounds have not been evaluated for delignification, most likely due to their low acidity. Here we demonstrate that the simple, solid dicarboxylic acid maleic acid (MA) has hydrotropic properties sufficient to solubilize a substantial amount of wood lignin at approximately 100 °C under atmospheric pressure. MA has the following advantages over *p*-TsOH: (1) it is a weaker acid (pK_a = 1.9) and much less corrosive, especially at elevated temperatures, and so reduces capital cost for distillation, (2) it has a much higher MHC of approximately 25 wt% as compared to 11.5% for *p*-TsOH, which reduces water usage for lignin precipitation, (3) it has a lower solubility of approximately 32 wt% as compared to more than 40 wt% for *p*-TsOH at 20 °C, which can make acid recovery easy and (4) it is an additive for cosmetics and has CFR (Code of Federal Regulations) title 21 GRAS (generally regarded as safe) status, so trace amounts of MA retained on cellulosic fibers will not cause safety concerns. Therefore, we believe that the present study offers very positive progress in biorefineries.

The objectives of the present study are to: (1) evaluate the performance of maleic acid hydrotropic fractionation (MAHF) for fractionating birch wood, (2) characterize the dissolved lignin chemical structure and mode of modification by MA using nuclear magnitic resonance (NMR) spectroscopy, (3) characterize physical properties of the lignin for potential valorization and (4) examine the impact of esterification of both the lignin and cellulose on the processibility of the dissolved lignin and fractionated cellulosic water insoluble solids (WIS). The overall goal is to provide fundamental understanding and performance information of MAHF for developing economically feasible and sustainable plant biomass biorefineries.

Results and discussion

Wood fractionation by maleic acid

Air-dried birch wood (15% moisture content) was Wiley-milled to 30 mesh and then fractionated using MA solution at a wood to MA solution ratio of 1 : 10 (w/w) according to the schematic flow diagram shown in Fig. 1. Fractionation runs were labeled as M*xx*T*yy*t*zz* to represent MA concentration of *xx* wt% at *yy* °C for *zz* min, as listed in Table S1.† The minimal hydrotropic concentration (MHC) of MA was determined to be 25 wt%

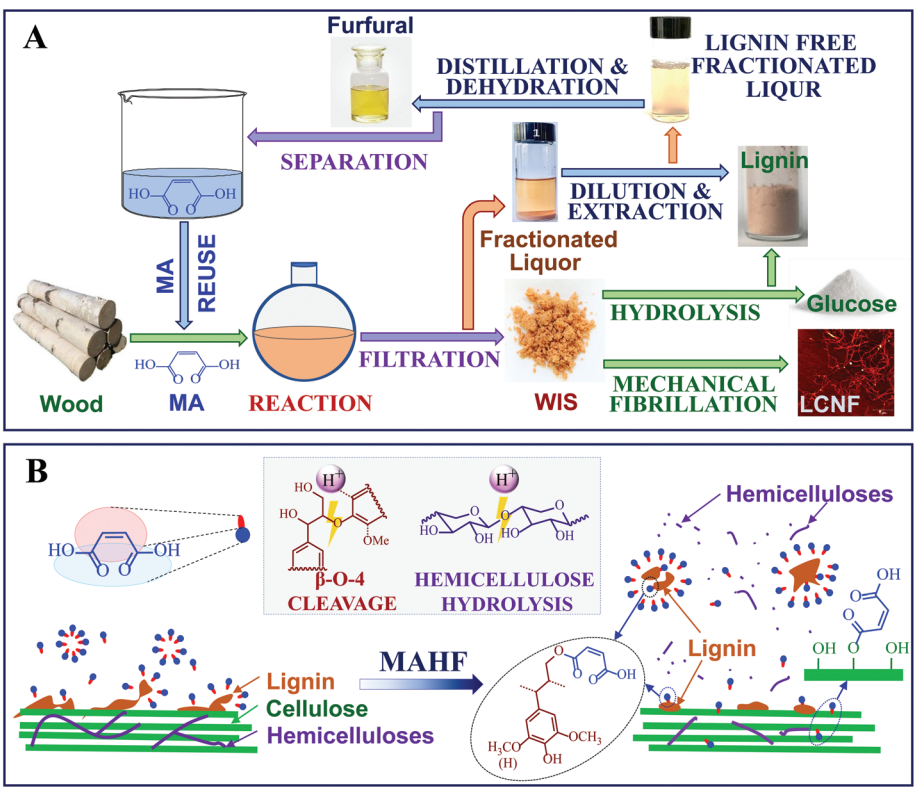

Fig. 1 Schematic flow (A) and hypothesized mechanism (B) diagrams show recyclable MA as an acid hydrotrope to fractionate wood for producing carboxylated lignin with a low degree of condensation, lignin-containing cellulose nanofibrils, and furfural.

from the conductivity of MA solutions (Fig. S1†),[32] which is more than double the MHC of *p*-TsOH of 11.4 wt%[22] and, therefore, beneficial for reducing water usage during precipitation of the dissolved lignin.

Dissolutions of lignin and hemicelluloses were higher with increasing fractionation severity, while cellulose loss was only mildly affected. For example, with increasing MA concentration from 50% to 70%, lignin and xylan dissolutions increased from 24.6% to 46.2% and 36.0% to 57.5%, respectively, while cellulose dissolution increased but remained low from 6.7% to 13.7%, after 60 min fractionation at 80 °C as shown in Fig. 2A. Similarly, on increasing the temperature from 80 °C to 100 °C, cellulose dissolution was increased from 6.8% to 16.5%, while lignin and xylan removal was increased from 24.6% to 49.4% and 36% to 70.1%, respectively, after 60 min reaction at a MA concentration of 50 wt% (Fig. 2B). These results suggest that both high acid concentration and high temperature are very favourable for lignin and hemicellulose dissolution with significant preservation of cellulosic fibers. However, increasing the reaction time from 30 to 120 min at an acid concentration of 50 wt% and 100 °C did not substantially increase lignin or xylan dissolution, *i.e.*, from 48.5% to 55.4% and 69.0% to 72.1%, respectively, but did significantly increase cellulose dissolution from 5.5% to 21.4% (Fig. 2C). Therefore, a short fractionation time is preferred and, as will be demonstrated later, results in a significantly less condensed lignin. The percentage of xylan solubilized as xylose in the fractionation liquor ranged from 11% to 66%, depending on fractionation severity (Table S1†).

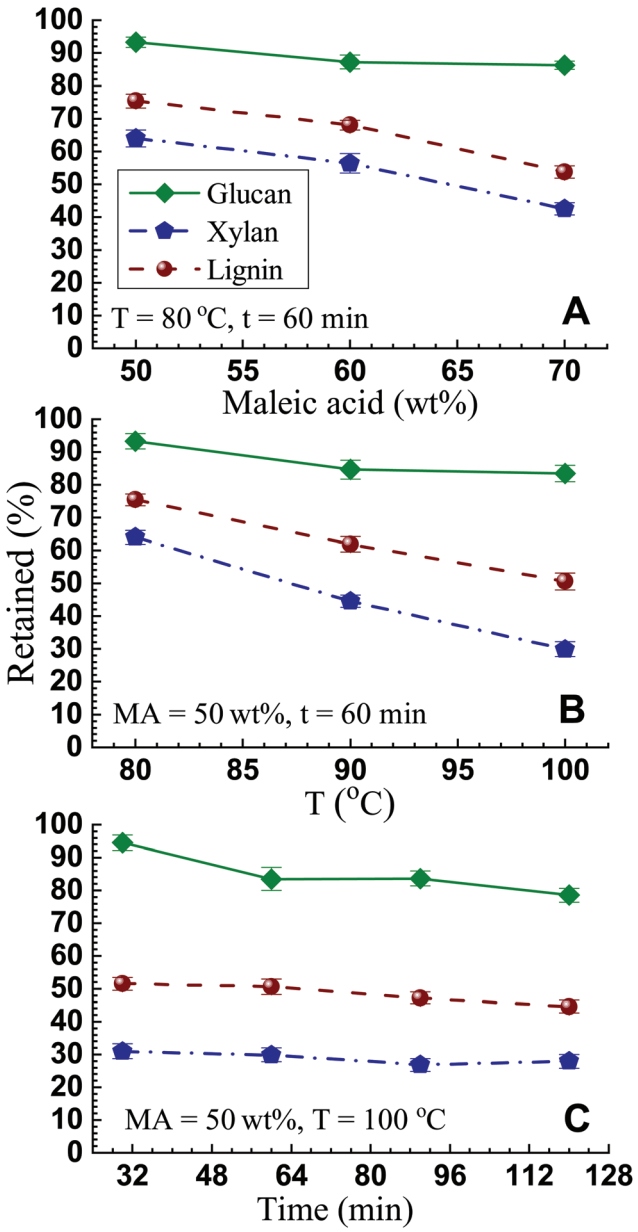

Fig. 2 Effects of maleic acid hydrotropic fractionation conditions on birch wood component retained on water insoluble solids (WIS). A: Maleic acid concentration; B: temperature; C: time.

Dissolved lignin esterifciation and characterization

2D ^{1}H–^{13}C HSQC NMR analysis of MWL and dissolved lignin from MAHF under different conditions was carried out and the relative percentage of substructures was calculated by integrating the crosspeak contours. Assignment of the main lignin substructures and linkages was made according to the literature.[33,34]

Under mild fractionation conditions, such as M50T80t60 (Fig. 3), the dissolved lignin contained a significant amount of carbohydrates which indicates that chemical bonds between lignin and polysaccharides were not completely cleaved, and the β-O-4 aryl ether linkages were also highly preserved being essentially the same as MWL (Table 1). The S/G ratio was slightly higher (increased from 4.5 of MWL to 4.9) probably because the guaiayl-rich lignin being more branched with a higher degree of polymerization is less solubilized under these mild fractionation conditions.[35] Nonetheless, it has a significantly lower molecular weight of 3958 Da than MWL's 14 832 Da due to substantial depolymerization by MA, in agreement with observations made using a strong acid hydrotrope *p*-TsOH hydrotrope under flow-through conditions.[8]

Increasing fractionation severity to M70T80t60 substantially reduced the carbohydrate content, increased the S/G ratio from 4.9 to 9.4, decreased β-O-4 from 64.5% to 43.3% and further decreased M_w to 2245 Da. Increasing fractionation severity again to M50T100t60 produced dissolved lignin showing almost no carbohydrates (Fig. 3), and increased the S/G ratio to 10.7, and β-O-4 and M_w were further reduced to 27.1% and 1641 Da, respectively.

We noted that the dissolved lignin from more severe fractionation conditions had additional strong signals in the aromatic region at $\delta C/\delta H$ 127.8/6.2 and 133.2/6.4 ppm and in the aliphatic region at 64.2/4.2, labeled Eγ(MA) in Fig. 3, that were not observed in the lignin under mild fractionation M50T80t60 conditions. In order to make these assignments, model compound guaiacylglycerol-beta-guaiacyl ether (GG) was reacted with MA under M60T100t60 conditions. GG condensation under acidic conditions produced 3,3-bis(4-hydroxy-

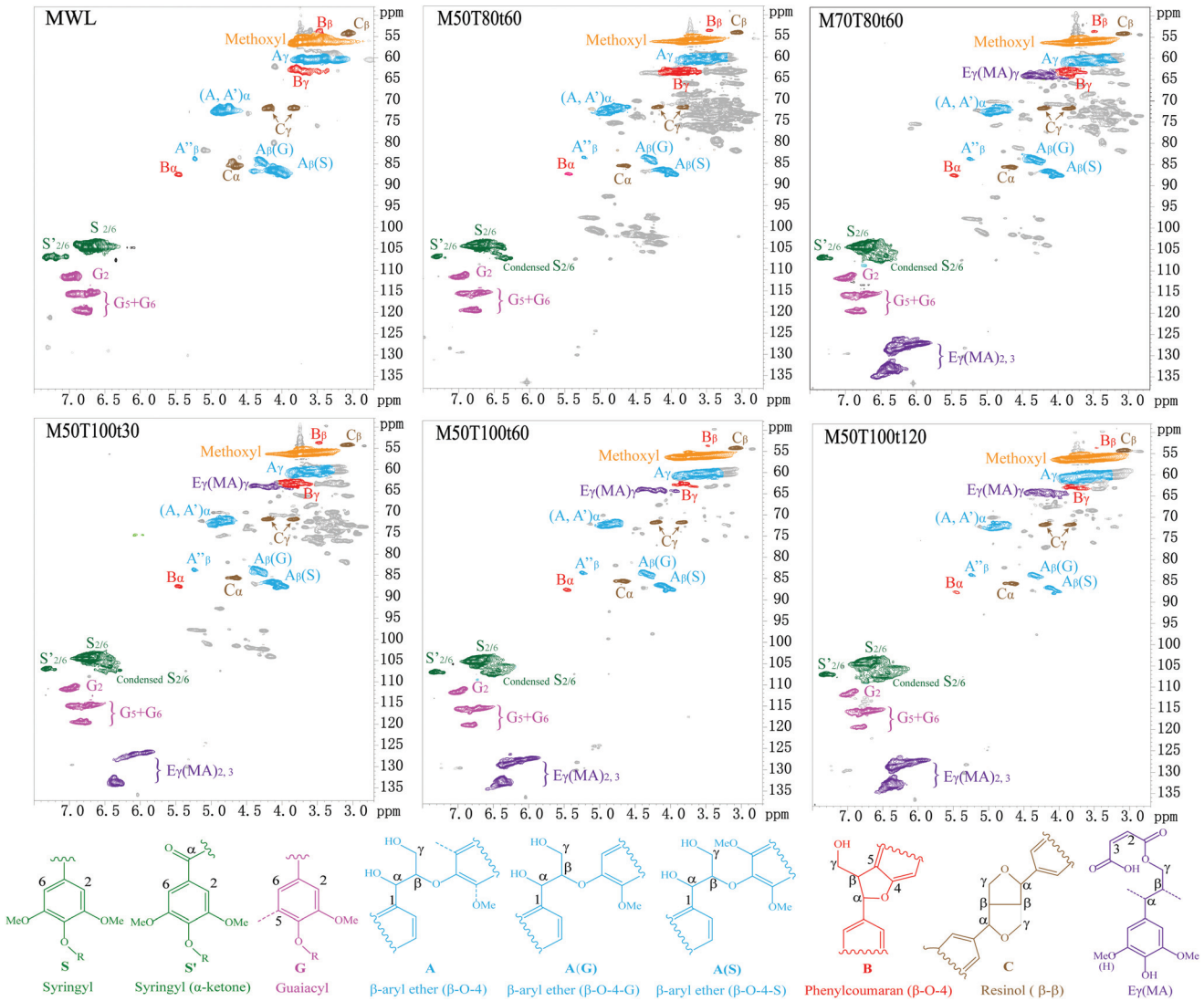

Fig. 3 2D $^{1}H-^{13}C$ HSQC NMR spectra of MWL and MAHF dissolved lignin. Eγ(MA) is the S or G unit lignin with γ-OH maleated.

Table 1 Structural characteristics (interunit linkages, aromatic units, and S/G ratio) of MAHF dissolved lignin from integrating $^{1}H-^{13}C$ correlation peaks in the HSQC spectra (the condensed $S_{2/6}$ is abbreviated as S_{Cond})

Sample	Ligin yield (%)	$S_{2/6}$	$S'_{2/6}$	S_{Cond}	S	G	S/G	β-O-4 (%)	β-5 (%)	β–β (%)	M_n	M_w	M_w/M_n
MWL	100	25	1.3	—	13.8	3.1	4.5	64.6	1.2	10.6	3227	14 832	4.6
M50T80t60	24.6	23.4	0.8	0.9	13.0	2.6	4.9	64.5	0.6	8.0	1886	3958	2.1
M70T80t60	46.2	21.5	0.8	4.4	15.5	1.6	9.4	43.3	0.5	7.2	1396	2245	1.6
M50T90t60	38.1	22.1	0.8	0.5	12.0	2.2	5.5	67.3	0.8	8.8	1858	3710	2.0
M50T100t30	48.5	20.9	0.7	2.6	13.4	1.8	7.7	54.1	0.2	7.8	1340	2380	1.8
M50T100t60	49.4	19.4	1.2	6.4	16.7	1.6	10.7	27.1	0.8	7.0	1109	1641	1.5
M50T100t120	53.4	16.2	1.2	9.3	18.0	1.0	18.4	16.1	0.1	4.9	1041	1420	1.4

3-methoxyphenyl)propane-1,2-diol (CD) as observed from the signals of CD_α, CD_β and CD_γ in Fig. 4A.[36] Previous NMR studies demonstrated that GG is esterified by formic acid and acetic acid at the γ-position with aliphatic HSQC signals for γ ($^{13}C-^{1}H$) at 63.5/(3.83, 4.30) and 62.1/(4.23, 4.43) ppm,[36–38] respectively. Corresponding signals from the GG–MA reaction product were observed at 63.6/(4.03, 4.39), as shown in Fig. 4A. Additionally, after reaction with GG, the MA signal at 130.8/6.3 ppm disappeared and 2 strong peaks appeared at $\delta C/\delta H$ 128.0/6.2 and 132.9/6.4 ppm, also consistent with esterification and presumably at the γ-position because the primary ester is more stable.[39]

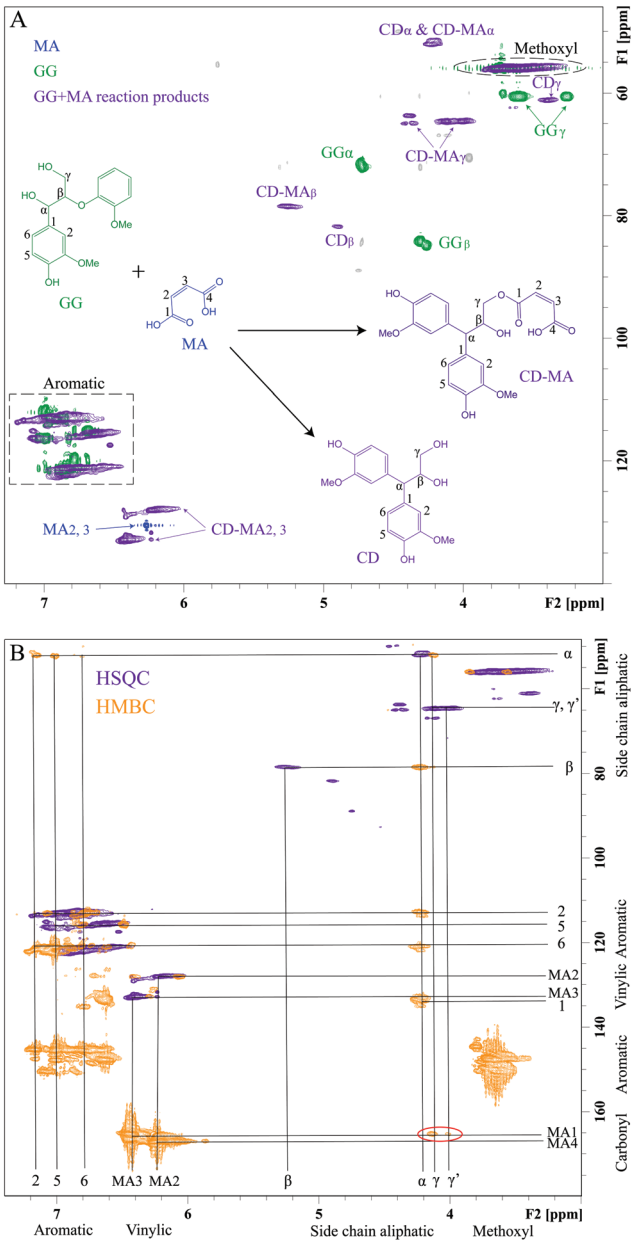

Fig. 4 A: 2D $^{1}H-^{13}C$ HSQC NMR spectra of MA, GG and GG–MA; B: 2D $^{1}H-^{13}C$ HSQC (purple) and 2D $^{1}H-^{13}C$ HMBC (orange) of GG–MA.

A long-range HMBC was performed for the GG–MA reaction product to verify esterification at the γ-position. As circled in Fig. 4B, the γ protons clearly show a 3-bond correlation to the C1 carbonyl of MA.

The hydroxyl groups in WML and the MAHF dissolved lignin were quantitatively analyzed by ^{31}P NMR (Fig. 5) according to a method previously described in ref. 10. MWL has the highest aliphatic OH content of 3.88 mmol g^{-1}, as listed in Table 3. MAHF reduces aliphatic OH, with the lignin from M50T100t60 (extended fractionation of 60 min) having the least aliphatic OH signal (Fig. 5) and content of 1.77 mmol g^{-1} (Table 2), suggesting that more aliphatic OH groups were substituted by MA with increasing reaction severity, which was also observed in $^{1}H-^{13}C$ HSQC spectra (Fig. 3). No significant change in the guaiacyl OH signal was observed in the dissolved lignin because MA does not directly esterify the phenolic hydroxyl group.[40,41] Only under the most severe condition (M50T100t60), 5-substituted OH in dissolved lignin was significantly higher than that in MWL (Table 2), which strongly suggests a less condensed lignin structure for most runs with a short reaction time of 30 min.[42]

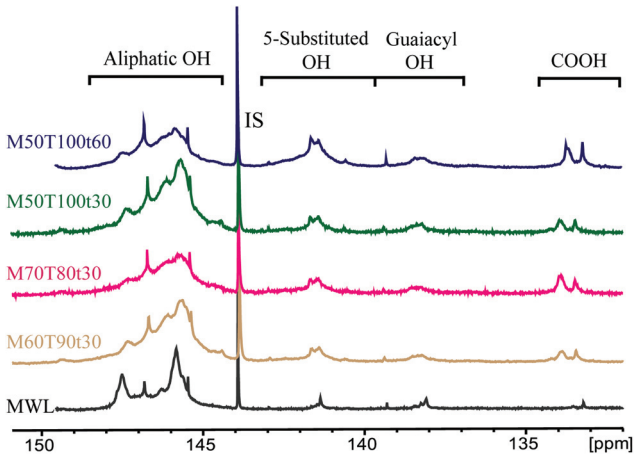

Fig. 5 Quantitative ^{31}P NMR spectra of the phosphitylated MWL and MAHF dissolved lignin under different conditions.

Table 2 Quantification of the functional groups in lignin by ^{31}P NMR spectroscopy

Sample	Aliphatic OH (mmol g^{-1})	5-Substituted OH (mmol g^{-1})	Guaiacyl OH (mmol g^{-1})	COOH (mmol g^{-1})
MWL	3.88	0.33	0.25	0.12
M60T90t30	3.06	0.53	0.23	0.39
M70T80t30	3.02	0.50	0.21	0.61
M50T100t30	3.24	0.53	0.25	0.45
M50T100t60	1.77	0.90	0.31	0.54

The carboxyl group content in dissolved lignin also increased with increasing fractionation severity (Table 2) due to esterification with MA in addition to oxidation of hydroxyl and carbonyl groups during delignification,[43] with lignin from M70T80t30 having the highest carboxyl content of 0.61 mmol g^{-1} because the esterification reaction always proceeds further with less water at high MA concentrations. The carboxyl group content in all dissolved lignin samples is higher than that reported for cellulose when lignin-free cellulosic fibers were reacted with dicarboxylic acids under similar or more severe reaction conditions.[44,45] Carboxylated lignin with a low degree of condensation is advantageous for high value valorization due to its ability to be modified for various applications.[46,47]

The less condensed structure of dissolved lignin from MAHF can also be indirectly deduced from the color of the lignin as shown in Fig. 6. Under mild conditions with almost

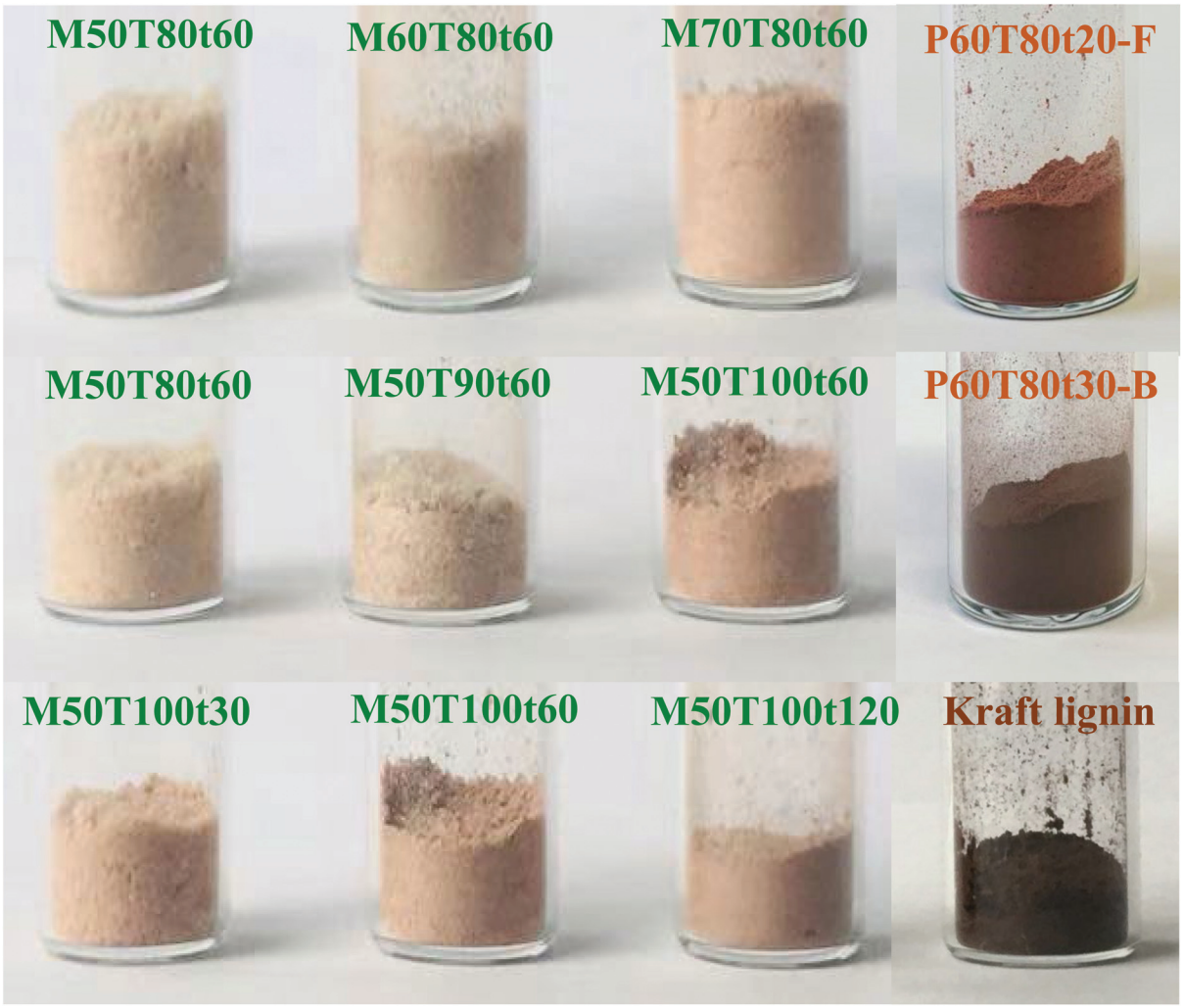

Fig. 6 Images show the color of dissolved wood lignin from MAHF under various conditions in comparison with lignin from AHF using *p*-TsOH and kraft pulping.

100% retention of β-O-4, such as M50T80t60 and M50T90t60, the lignin is very light tan in color. Even under the most severe condition tested, M50T100t120, the MAHF lignin remains tan colored, in stark contrast to lignin obtained from kraft pulping which has a very dark color. The MAHF lignin is also much lighter than lignin from *p*-TsOH AHF, which was pink/reddish-brown or brown as observed under flow-through and batch conditions, respectively. We expect that flow-through MAHF will also yield light colored lignin even under severe MAHF conditions, and will be investigated in subsequent studies.

MAHF water insoluble cellulosic solids

The discussion above only validated the esterification of dissolved lignin. However, it is plausible to assume that some of the undissolved lignin remaining on the WIS fraction is also esterified, especially under severe fractionation conditions. We evaluated the effectiveness of MAHF in mitigating recalcitrance to enzymatic processing of WIS by measuring enzymatic sugar productivity as shown in Fig. 7 using substrate enzymatic digestibility (SED), defined as the percentage of WIS glucan enzymatically saccharified into glucose. For the range of fractionation conditions studied, increasing MA concentration (Fig. 7A) and fractionation temperature (Fig. 7B) improved SED. This is simply due to the improved dissolution of hemicelluloses and lignin as shown in Fig. 2A and B, respectively, which improved substrate cellulose accessibility to cellulase.[48] The control sample shown in Fig. 7A–C is the unfractionated birch. At a MA concentration of 50 wt% and 100 °C, SED also increased with increasing fractionation time up to 90 min but decreased with a much extended 120 min fractionation time (Fig. 7C). Also, the 120 min fractionation time did not further increase xylan dissolution and only minimally increased delignification (Table S1†). Moreover, prolonged fractionation increased lignin condensation which tends to deposit lignin onto the substrate surface and increases nonproductive binding of cellulase. It is also possible that the extended reaction in concentrated MA solution may increase substrate cell-

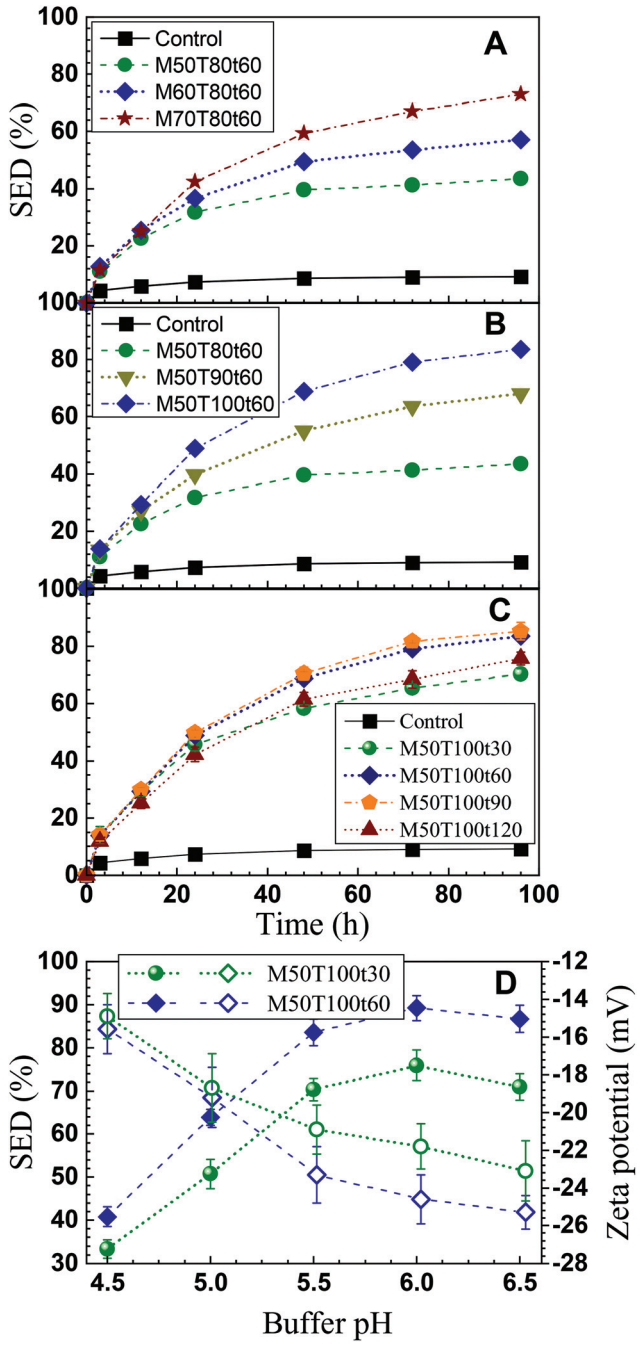

Fig. 7 Effects of maleic acid hydrotropic fractionation conditions and hydrolysis buffer pH on WIS enzymatic digestibility (CTec3 loading = 10 FPU g^{-1} glucan; buffer pH = 5.5 for A–C). A: Fractionation time; B: acid concentration; C: fractionation temperature; D: buffer pH.

ulose consolidation or crystallization[49–51] to become more recalcitrant to enzymatic hydrolysis.

Our earlier study showed that nonproductive binding of cellulase to substrate lignin can be substantially reduced through electrostatic repulsive interactions by elevating the pH during enzymatic hydrolysis.[52,53] For the two WIS samples produced in this study, M50T100t30 and M50T100t60, their SED values increased with increasing pH of the hydrolysis buffer solution until reaching a maximum at pH = 6.0, and then decreased with further increasing pH (Fig. 7D). The surface charge measured by zeta-potential (absolute value) of the two substrates increased continuously with the increasing pH of buffer solution (Fig. 7D), suggesting increasing electrostatic repulsion to cellulase because most cellulase has a pI around 5.0[54] and becomes more negatively charged as buffer pH exceeds its pI. This electrostatic repulsive interaction is attributed to lignin carboxylation (esterification) as discussed above. Lignin carboxylation plays a similar role to lignin sulfonation when lignocelluloses are fractionated using sulfite, which increases lignin surface charge especially under elevated pH.[52] When pH was further increased beyond 6.0, the efficacy of cellulase on cellulose (typically optimum at pH = pI of cellulase) decreased more than the positive effect from reducing nonproductive binding.

To assess the performance of MAHF for removing lignocellulose recalcitrance to enzymatic saccharification, the SED of M50T100t60 was compared with that for other fractionation/pretreatment methods reported in the literature. As listed in Table S2,† MAHF produced equivalent or better SED with a low cellulase loading of 10 FPU g^{-1} glucan.

Lignocellulosic nanofibrils (LCNFs) have attracted great interest recently for their renewability, large surface area, high strength, and optical properties.[55,56] Lignin provides LCNFs some unique properties such as UV protection, hydrophobicity, *etc.*[57,58] Producing LCNFs from wood through mechanical fibrillation, however, is expensive due to strong hydrogen bonding and the tight cell wall structure. During MAHF, the cellulose is also esterified, though the lignin was more easily esterified as discussed earlier,[59] resulting in a carboxylated WIS. Its carboxyl content ranged from approximately 0.08 to 0.13 mmol g^{-1}, much lower than that in disolved lignin (Table 2) partially due to a low lignin content in the LCNF sample.

The fractionated WISs from M60T90t30, M50T100t30, M50T100t60 and M70T100t15 were directly fibrillated through microfluidization. AFM measurements indicate that the LCNFs have a length of several micrometers with the heights or diameters between 4 and 18 nm (Fig. 8A and B). Free lignin nanoparticles (bright spots) are observable in AFM images. In general, increasing fractionation severity improved carboxylation and surface charge and reduced the LCNF diameter. For example, with extending fractionation from 30 to 60 min at a MA concentration of 50 wt% and 100 °C, the carboxyl group content of LCNFs was increased from 0.105 to 0.134 mmol g^{-1} (Table 3), and the average diameter was reduced from 9.1 to 6.5 nm. At a MA concentration of 70 wt% and 100 °C, a 15 min fractionation resulted in very fine LCNFs of average diameter 7.7 nm. Compared with cellulose nanofibrils (CNFs) obtained by directly hydrolyzing bleached pulp fibers using MA,[45] the LCNFs obtained in this work have a similar diameter of several to ten nanometers as shown in Fig. 8, indicating that the presence of lignin in WIS has no negative influence on fibrillation which is in contrast to current conventional understanding.[60]

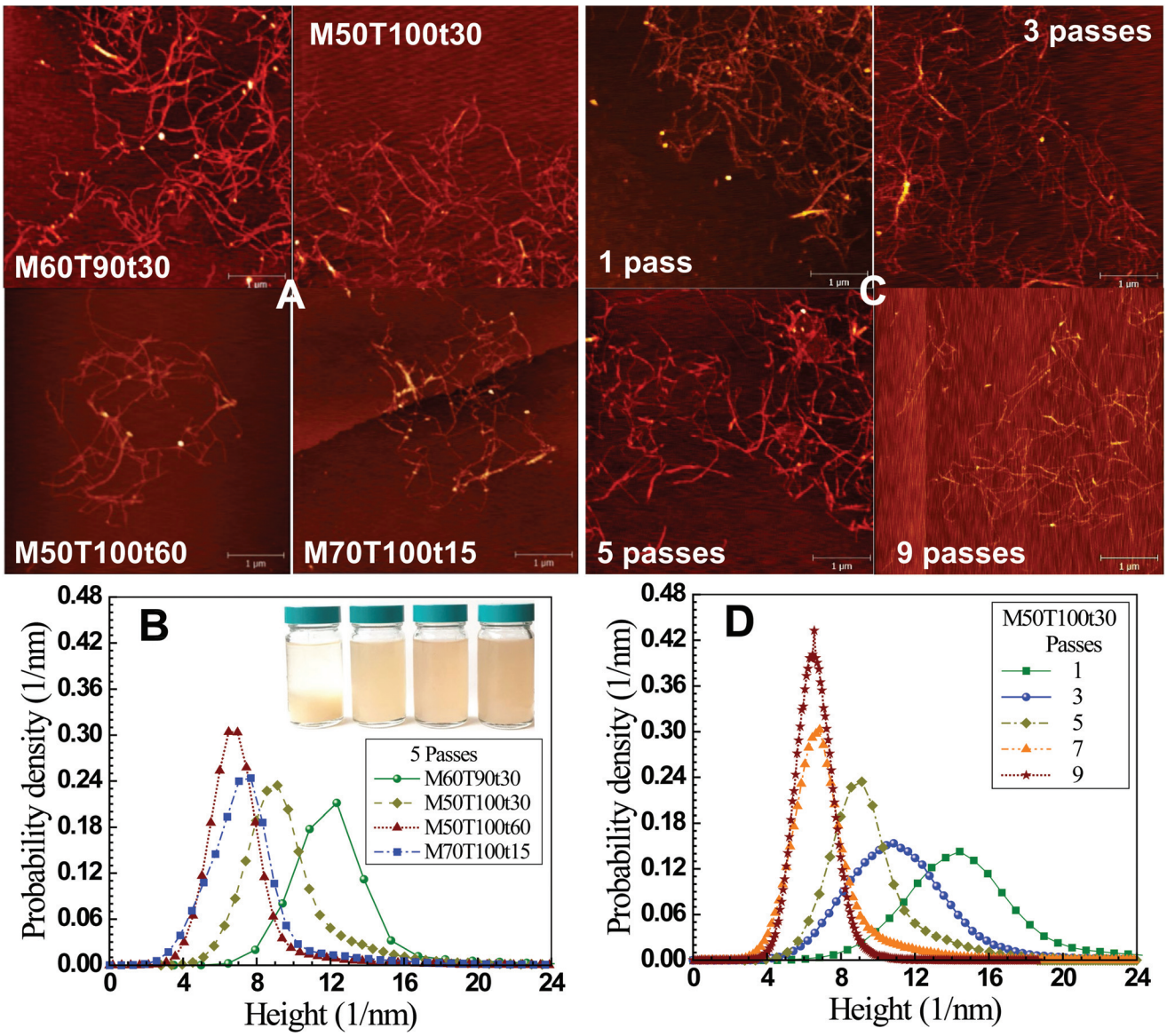

Fig. 8 Maleic acid hydrotropic fractionation conditions (A and B) and extent of mechancial fibrillation (C and D under M50T100t30) on the resultant LCNF morphology and fibril height distribution observed by AFM. A and C: AFM topographic images of LCNFs; B and D: height distributions.

These LCNFs have a high lignin content between 16 and 18% (Table S1†) and good surface charge (zeta potential) ranging from −41 to −46 mV as listed in Table 3. The electrostatic repulsion from the surface carboxyl groups enhanced fibril separation during mechanical fibrillation through enhancing the "lubrication effect" of residual lignin.[61,62] The carboxylated LCNFs are also favorable for further surface modifications for a variety of applications.[63,64]

Table 3 Carboxyl content and zeta potential of LCNFs obtained from MAHF under different conditions

LCNF sample	COOH groups (mmol g^{-1})	Zeta potential (mV)
M60T90t30	0.084 ± 0.008	−41.4 ± 1.9
M50T100t30	0.105 ± 0.012	−43.4 ± 0.8
M50T100t60	0.134 ± 0.009	−46.3 ± 1.4
M70T100t15	0.122 ± 0.013	−44.1 ± 0.9

To further illustrate the effect of lignin carboxylation on nanofibrilation, we compared the fibrillation of WIS from M50T100t30 with WIS without carboxylation from AHF using *p*-TsOH.[25] First we noted that increasing the extent of fibrillation (the number of passes through the 87 μm chamber) reduced both the extent of LCNF entanglement and LCNF diameter (height measured by AFM) as shown in Fig. 8C and D, respectively, in agreement with that reported for fibrillation of WIS from AHF using *p*-TsOH.[25] Specifically, the average height (diameter) was decreased from 14.4 nm to 10.8, 9.1, 6.9 and 6.6 nm, as the number of passes was increased from 1 to 3, 5, 7 and 9, respectively. Fibrillation of the same birch wood frac-

Table 4 Comparisons of the effect of *p*-TsOH and MA fractionations on the resultant LCNF mean sizes

WIS	LCNF passes	Average height (nm)	Standard deviation (nm)
***p*-TsOH**: P50T80t20	1	70.0	5.6
Lignin: 16%	3	65.2	8.0
Xylan: 15%	5	51.1	2.4
Cellulose: 59%	7	22.5	2.0
	9	14.3	1.2
MA: M50T100t30	1	14.4	2.4
Lignin: 15%	3	10.8	1.9
Xylan: 11%	5	9.1	1.4
Cellulose: 58%	7	6.9	1.1
	9	6.6	0.9
***p*-TsOH**: P65T80t20[a]	5	29.4	1.3
***p*-TsOH**: P80T80t20[a]	5	15.3	1.6

[a] Lignin, xylan, and cellulose contents for P65T80t20 and P80T80t20 are: 12% and 7%, 14% and 12%, 62% and 68%, respectively.

tionated using *p*-TsOH without lignin carboxylation, however, resulted in much greater average diameters under similar or higher delignification as compared in Table 4. This clearly demonstrates that the surface carboxyl groups derived from MAHF favorably facilitated nanofibrillation. Although the WIS from M50T100t30 had a lignin content of 15.4%, after only one pass through microfluidization it was readily fibrillated to a very fine diameter of approximatley 14 nm, smaller than those reported in the literature using other methods without lignin carboxylation.[61,65] This further supports the hypothesis that lignin carboxylation (esterification) 'lubricates'[61,62,66] to reduce hydrogen bonding for improved nanofibrillation.

LCNF surface charge from lignin surface carboxylation (esterification) also improved the stability of four LCNFs. 0.2% aqueous dispersions of the LCNFs were allowed to stand in a cold storage at 4 °C for two weeks. Only LCNF from M60T90t30 with the least negative charge (Table 3) precipitated (Fig. 8B and Fig. S2†). The other three samples remained uniformly dispersed.

Furfural production and MA recovery

To demonstrate furfural production from dissolved xylan, the fractionation liquor from M50T100t30 was diluted to a MA concentration of 15 wt%, the precipitated lignin from dilution was filtered and the colloidal lignin was further extracted using *n*-pentanol (the chemical structure of the *n*-pentanol extracted lignin is similar to that of the dilution precipitated lignin as compared in Fig. S3†). The lignin-removed diluted fractionation liquor was then directly used without pre-concentration for producing furfural through distillation. It should be noted that small amounts of xylose and MA remained in the WIS due to incomplete washing of WIS through simple dilution to 15 wt%, and were not accounted for here. MA has been shown to be an effective catalyst to dehydrate xylose into furfural.[67,68] The reported furfural yields were calculated based on the amount of dissolved xylan by MAHF. Total furfural includes furfural from dehydration in the distillate and the amount in the fractionation liquor produced during fractionation. We found that the concentration of furfural in the distillate first increased and then decreased with fractionation temperature (Table 5). Increasing temperature favors dehydration of xylose, but degradation side reactions can take place at elevated temperatures.[69] The optimal temperature was 180 °C with a maximal yield of 70.1%.

The MA concentration in the distilled liquor was approximately 50 wt% and was used directly for the second cycle of fractionation (Fig. S4†) using the same amount of birch wood after spiking a small amount of fresh MA, equivalent to 5% of the original applied amount, to compensate for any MA lost in the process in the previous cycle, including those remaining in the WIS which can be estimated to be approximately 1–2% due to incomplete washing based on the previous washing study using *p*-TsOH.[23] As listed in Table 6, the yields and chemical composition of the WIS from the cycle using fresh MA are indifferent (within the measurement error margins) from the corresponding values from the two runs using recovered MA. Because xylose was dehydrated into furfural and distilled along

Table 5 Effect of distillation temperature on furfural yield from dissolved xylan

Temperature (°C)	Furfural in distillate (g L^{-1})	Furfural in the fractionation liquor (g L^{-1})	Dehydration furfural yield (%)	Total furfural yield (%)
160	1.54 ± 0.09	0.86 ± 0.04	29.6	37.9
170	2.89 ± 0.09	0.73 ± 0.11	55.7	62.6
180	3.23 ± 0.13	0.83 ± 0.08	62.2	70.1
190	3.06 ± 0.17	0.85 ± 0.09	58.8	67.0

Table 6 Comparisons of chemical compositions of WISs from MAHF runs using fresh and recycled MA

	Fractionated WISs				Fractionation liquor		
	Yield (%)	Glucan (%)	Xylan (%)	Lignin (%)	Glucose (g L^{-1})	Xylose (g L^{-1})	Acetic acid (g L^{-1})
First	64.7 ± 1.1	57.4 ± 1.4	11.0 ± 0.9	15.4 ± 1.1	0.20	9.46	2.68
Second	63.4 ± 2.1	58.2 ± 2.9	10.6 ± 1.0	14.8 ± 0.9	0.42	10.2	2.71
Third	65.3 ± 1.9	56.5 ± 1.8	11.5 ± 1.2	16.0 ± 0.5	0.60	9.11	2.42

with acetic acid, the measured dissolved xylose and acetic acid concentrations in the two spent liquors from the recycling runs were essentially the same as those from the fresh fractionation liquor, but glucose accumulation was observed with recycling, *i.e.*, glucose concentration in the fresh liquor was 0.2 g L^{-1} and increased to 0.4 and 0.6 g L^{-1} in the two subsequent recycling runs. The accumulated glucose can potentially be recovered as levulinic acid through dehydration[70] but was not attempted in this study.

Conclusion

This study identified maleic acid (MA) as an effective hydrotrope with a minimal hydrotropic concentration of approximately 25 wt% for efficient delignification of wood at atmospheric pressure and approximately 100 °C. 2D ^{1}H–^{13}C NMR HSQC and HMBC analyses of the dissolved lignin and lignin model compound reaction product with MA demonstrated esterification at the γ-OH group. The resultant carboxylation of dissolved lignin and water insoluble solids (WIS) depended on the severity of MA fractionation conditions. The WIS carboxylation is beneficial because it reduces nonproductive cellulase binding which enhances enzymatic processing of WIS through pH mediation (elevated pH). It is also advantageous for producing lignin containing cellulose nanofibrils (LNCF) through mechanical fibrillation because lignin carboxylation enhanced the lignin lubrication effect for fibrillation. MA hydrotropic fractionation (MAHF) produces dissolved lignin with a low degree of condensation and a very light color which is dispersible due to carboxylation making it amenable to a variety of applications. The dissolved xylose can be dehydrated into furfural and the MA can then be reused. Preliminary studies indicated that MA recovery of at least 95% can be achieved. Compared to strong acid hydrotropes such as *p*-toluenesulfonic acid, MA is less corrosive and has a higher MHC for more favorable acid recovery and reuse and has GRAS status, all of which demonstrate a notable step forward in biorefineries.

Materials and methods

Materials

Anhydrous maleic acid (MA) was purchased from Sigma-Aldrich (St Louis, MO. USA). All chemicals were used as received. Birch wood chips were hammer-milled using a 4.8 mm screen, then Wiley-milled to 30 mesh and dried at room temperature for 24 hours to approximately 15% moisture content. The dried material was stored in a refrigerator for later use. Commercial complex cellulose, Cellic® CTec3, was complimentarily provided by Novozymes North America (Franklinton, NC, USA).

Fractionation of wood by MA

30 g aqueous MA solutions with a concentration range of 30–70 wt% were prepared in 100 mL Duran Laboratory glass bottles by solubilizing desired amounts of MA in deionized (DI) water. Each bottle was placed on a temperature-controlled shaker (Model 4450, Thermo Scientific, Waltham, USA) at 250 rpm to promote dissolution of MA. 3 g in oven dry (OD) weight of the Wiley-milled birch sample was placed into each 30 g prepared MA solution with continuous shaking at a designated temperature for a preset reaction time. At the end of each fractionation, the spent MA liquor was separated through filtration. The solids were washed using DI water until the filtrate was diluted to 15 wt% MA to precipitate lignin. After centrifugation, the precipitated lignin was dialyzed in DI water for one week and freeze dried. Then 20% (v/v) of *n*-pentanol was added to the solution to extract the residual lignin (Fig. S3†) that is compared with dilution precipitated lignin. The lignin-removed solution was used for furfural production and MA recyclability. The washed WIS were analyzed for chemical compositions.

Chemical compositional analyses

The chemical composition of the WIS was determined by conventional two-step acid hydrolysis, as described previously.[71] The chemical composition of the spent liquors was analyzed using a HPLC system (Ultimate 3000, ThermoFisher Scientific), as described previously.[24,72] Specifically, xylose, furfural and acetic acid were chromatographically separated using a BioRad Aminex HPX-87H column (300 mm × 7.8 mm) operated at 50 °C and detected by a refraction index detector (RI-101, Shodex).

Mechanical fibrillation of fractionated lignocellulosic solids

The washed WIS from each run was first dispersed in DI water and then placed in a disintegrator (TMI, Ronkonkoma, NY, USA) at 0.5 wt% for 20 000 revolutions. The suspension was then directly fed into a microfluidizer (M-110EH, Microfluidics Corp., Westwood, MA, USA) to mechanically fibrillate the fibers at 120 MPa for 5 passes through two chambers in series of diameters of 200 and 87 μm.

Atomic force microscopy (AFM) imaging

The morphologies of lignocellulosic nanofibril (LCNF) samples were observed by AFM imaging. Aqueous LCNF suspensions of approximately 0.01 wt% were dispersed under sonication and deposited on a mica surface, and then air-dried at room temperature. The LCNFs were imaged in the vibrating tapping mode using an AFM system (CS-3230, AFM Workshop, Signal Hill, CA, USA). Height distributions of LCNFs were obtained by analyzing the AFM measured topography using Image-Pro Plus software (Media Cybernetics, Silver Spring, MD, USA).

Enzymatic hydrolysis

Enzymatic hydrolysis of WIS was conducted using 2% (w/w) solids with acetate buffer (50 mM) in a shaker at 50 °C and 150 rpm. Elevated pH was applied to reduce nonproductive binding of cellulase to substrate lignin through electrostatic interaction.[52,53] Cellulase CTec3 loading was 10 FPU g^{-1}

glucan. Aliquots of 1 mL of hydrolysate were taken at different times to obtain time-dependent saccharification. Glucose in enzymatic hydrolysates was measured with a commercial glucose analyzer (YSI 2700S, YSI Inc., Yellow Springs, Ohio). All data points were the average of two analyses.

Furfural production from dissolved xylan

After lignin precipitation through dilution, the diluted fractionation liquors of 15 wt% were directly used to produce furfural from the dissolved xylan without additional catalysts (*i.e.* using the MA in the diluted fractionation liquors). The reaction was conducted in a bomb digester heated in a sand bath, as described previously.[40,73,74] 30 mL of diluted fractionation liquor was dispensed into a reactor and heated to the set temperature for 10 min after sealing. The reaction was carried out for additional 10 min at the set temperature. Batch distillation of furfural was employed by opening a valve in the distillation line that is submerged in an ice water bath (Fig. S5†). The distillation flow rate was maintained at approximately 2 mL min^{-1}. The reaction was terminated after collecting 20 mL of condensate. The MA in the final liquid was then concentrated to approximately 50 wt% and used for the second cycle of fractionation after supplementing with 5% of the original amount of MA to compensate for acid losses primarily due to esterification of lignin and WIS. The furfural concentration of the distillate and the final liquor was analyzed by HPLC.

Preparation of MWL

Air-dried wood chips were milled to pass 30 mesh in a Wiley mill (Model No. 2, Arthur H. Thomas Co.). The dried wood powder was then milled in a vibratory ball mill (Retsch, PM 100) for 20 h. The ball-milled wood was dispersed in an aqueous dioxane solution with a volumetric concentration of 90% followed by mechanical stirring at 50 °C.[75] The wood loading was 4 g in 100 mL solution. After 24 h, the suspension was filtered and the solids were re-dispersed in fresh aqueous dioxane solution for additional 24 h. The liquid extracts were combined and then dried in a rotary vacuum evaporator to obtain crude MWL. The crude MWL was then dissolved in 90% acetic acid and precipitated by adding water and then dried to obtain MWL. For further purification, the MWL was dissolved in a mixture of 1,2-dichloroethane and ethanol (2 : 1), and precipitated by adding diethyl ether, followed by washing and drying.

2D ^{1}H–^{13}C NMR

2D ^{1}H–^{13}C NMR analysis of lignin was performed using a Bruker 500 MHz Avance III HD spectrometer equipped with a Prodigy (liquid N2-cooled) 5 mm gradient TCI (inverse configuration) $^{1}H/^{13}C/^{15}N$ cryo-probe.[23,26] Approximately 55 mg of purified lignin was dissolved in 0.5 mL of DMSO-d_6, referenced at 39.5/2.49 ppm. Heterogeneous single quantum correlation (HSQC) and heteronuclear multiple bond correlation (HMBC) experiments were performed using Bruker standard pulse programs hsqcetgpsisp 2.2 and hmbcgpl2ndqf, both with non-uniform sampling of 50%.

HSQC spectra were acquired using 40 scans and an inter-scan delay (D1) of 1 s for a total experiment time of 3 h, with a 12 ppm sweep width in F2 (^{1}H) using 1024 data points for an acquisition time (AQ) of 85 ms and a 215 ppm sweep width using 512 increments for AQ of 9.74 ms in F1 (^{13}C). Data processing used squared cosine-bell in F1 and F2, resulting in a 1024 × 1024 data matrix. Topspin 3.7p17 was used for interactive integration of 2D crosspeaks. Calculation of β-O-4, β–β, and β-5 amounts was described previously.

HMBC spectra were acquired using a long range evolution delay of 0.036 s corresponding to 14 Hz for J_{XH} (long range) and using 920 scans and an inter-scan delay of 1 s for a total experiment time of 10 h, with the same sweep widths as HSQC but 2048 and 256 data points in F2 and F1 respectively. Processing to a resultant 2056 × 512 data matrix used Gaussian Multiplier (GM) in F2 with LB = −40 and GB = 0.125 to favor sensitivity and QSINE squared in F1. ^{1}H–^{13}C HMBC correlates chemical shifts of protons and carbons separated by two and three bonds, with low pass filters eliminating the single quantum coherences observed in HSQC. As shown in Fig. 4B, H_β, H_2, H_6 and H_1 have significant coherent signals with C_α, while H_2 and H_3 in MA have strong coherent signals with C_1 and C_4 of MA. It should be noted that the C_1 carbonyl of MA has two distinct coherent signals with Hγ and Hγ′, indicating that MA was bonded at the γ-hydroxyl (esterification) rather than simply remaining as a mixture or a coordinated component in the GG–MA reaction product. Under mild fractionation conditions, for example M50T80t60, MA was hardly bonded onto lignin based on the HSQC spectrum in Fig. 3. Under more severe conditions with either increasing MA concentration, elevated temperature, or extended reaction time, such as M60T100t60 for the GG–MA reaction, MA bonding was prominent (Fig. 3).

Graphic figures were prepared using Adobe Illustrator from spectra exported from MestReNova/TopSpin in pdf format.

Lignin molecular weight determination using GPC

0.05 g of the freeze-dried lignin was dissolved in 2 ml of pyridine–acetic anhydride (1 : 1 by volume) solution. The solution was kept in a dark cabinet for 3 days at room temperature, and then added dropwise into 120 mL ice-cold DI water. After approximately 2 h, the solution was filtered. The precipitated lignin acetate was collected, washed with water, and then air-dried at 50 °C. The M_n and M_w of the acetylated lignin samples were measured on an ICS-3000 system (Dionex) with three 300 × 7.8 mm Phenogel 5U columns (10 000, 500, and 50 Å).[76] 2 mg of lignin acetate was dissolved in 2 mL THF without a stabilizer. 50 μL of the resulting solution was injected into the GPC columns at 30 °C with THF as the eluent. Lignin was analyzed by UV absorption using a variable wavelength detector at 280 nm. Polystyrene was used as the standard for calibration.

^{31}P NMR

For quantitative ^{31}P NMR analyses, 20 mg lignin was dissolved in anhydrous pyridine (500 μL) and deuterated chloroform (1.6 : 1, v/v) under stirring, followed by adding cyclohexanol

(100 μL, 10.85 mg mL^{-1}) as an internal standard and chromium(III) acetylacetonate solution (100 μL, 5 mg mL^{-1}) as the relaxation reagent[42] both in anhydrous pyridine and deuterated chloroform (1.6 : 1, v/v). The mixture was reacted with phosphitylating reagent (100 μL, 2-chloro-4,4,5,5-tetramethyl-1,3,2-dioxaphospholate, TMDP) for approximately 10 min and then transferred into a 5 mm NMR tube for subsequent NMR analysis.

Lignin model compound reaction

Guaiacylglycerol-beta-guaiacyl ether (GG) was used as the lignin model compound to investigate the lignin reaction mechanism in MA solution. 10 mg GG was dissolved in 100 μL of 60 wt% MA solution, and the reaction was carried out at 100 °C for 1 h. 1 mL of DI water was then added to precipitate the reaction product. The precipitate was washed with DI water to remove residual MA. After lyophilization, the product was dissolved in 0.5 mL of DMSO-d_6 for 2D ^{1}H–^{13}C HSQC and HMBC NMR analyses.

Conflicts of interest

Zhu and Gleisner are co-inventors of the maleic acid hydrotropic fractionation process.

Acknowledgements

This work was conducted while Cheng Cai was a visiting Ph.D student at the US Forest Service, Forest Products Laboratory (FPL). We acknowledge the financial support from the Chinese Scholarship Council (CSC) for Mr Cai's visiting program. We also like to acknowledge Fred Matt of FPL for conducting carbohydrate analyses and Daniel Yelle and Sally Ralph of FPL for helpful discussions. Huihui Wang, a visiting student, is acknowledged for recording ^{31}P NMR spectra at South China University of Technology. Prof. Xuejun Pan at the University of Wisconsin-Madison is acknowledged for allowing us to use his GPC system and helping us analyze lignin molecular weights.

References

1 H. Kopetz, *Nature*, 2013, **494**, 29.
2 J. Y. Zhu and X. J. Pan, *Bioresour. Technol.*, 2010, **101**, 4992–5002.
3 S. Tian, W. Zhu, R. Gleisner, X. J. Pan and J. Y. Zhu, *Biotechnol. Prog.*, 2011, **27**, 419–427.
4 C. E. Wyman, B. E. Dale, R. T. Elander, M. Holtzapple, M. R. Ladisch, Y. Y. Lee, C. Mitchinson and J. N. Saddler, *Biotechnol. Prog.*, 2009, **25**, 333–339.
5 S. M. Ewanick, R. Bura and J. N. Saddler, *Biotechnol. Bioeng.*, 2007, **98**, 737–746.
6 X. Pan, N. Gilkes, J. Kadla, K. Pye, S. Saka, D. Gregg, K. Ehara, D. Xie, D. Lam and J. Saddler, *Biotechnol. Bioeng.*, 2006, **94**, 851–861.
7 M. Iakovlev and A. van Heiningen, *ChemSusChem*, 2012, **5**, 1625–1637.
8 J. S. Luterbacher, J. M. Rand, D. M. Alonso, J. Han, J. T. Youngquist, C. T. Maravelias, B. F. Pfleger and J. A. Dumesic, *Science*, 2014, **343**, 277–280.
9 J. Y. Zhu, X. J. Pan, G. S. Wang and R. Gleisner, *Bioresour. Technol.*, 2009, **100**, 2411–2418.
10 R. Rinaldi, R. Jastrzebski, M. T. Clough, J. Ralph, M. Kennema, P. C. A. Bruijnincx and B. M. Weckhuysen, *Angew. Chem.,– Int. Ed.*, 2016, **55**, 8164–8215.
11 G. Gellerstedt and E. L. Lindfors, *Holzforschung*, 1984, **38**, 151–158.
12 P. J. Deuss, C. S. Lancefield, A. Narani, J. G. De Vries, N. J. Westwood and K. Barta, *Green Chem.*, 2017, **19**, 2774–2782.
13 S. Constant, H. L. J. Wienk, A. E. Frissen, P. D. Peinder, R. Boelens, D. S. Van Es, R. J. H. Grisel, B. M. Weckhuysen, W. J. J. Huijgen, R. J. A. Gosselink and P. C. A. Bruijnincx, *Green Chem.*, 2016, **18**, 2651–2665.
14 S. Van Den Bosch, W. Schutyser, R. Vanholme, T. Driessen, S. F. Koelewijn, T. Renders, B. De Meester, W. J. J. Huijgen, W. Dehaen, C. M. Courtin, B. Lagrain, W. Boerjan and B. F. Sels, *Energy Environ. Sci.*, 2015, **8**, 1748–1763.
15 M. V. Galkin and J. S. M. Samec, *ChemSusChem*, 2016, **9**, 1544–1558.
16 L. Shuai, Y. M. Questell-Santiago and J. S. Luterbacher, *Green Chem.*, 2016, **18**, 937–943.
17 N. Li, Y. D. Li, C. G. Yoo, X. H. Yang, X. L. Lin, J. Ralph and X. J. Pan, *Green Chem.*, 2018, **20**, 4224–4235.
18 C. S. Lancefield, I. Panovic, P. J. Deuss, K. Barta and N. J. Westwood, *Green Chem.*, 2017, **19**, 202–214.
19 A. Rahimi, A. Ulbrich, J. J. Coon and S. S. Stahl, *Nature*, 2014, **515**, 249–252.
20 J. S. Luterbacher, A. Azarpira, A. H. Motagamwala, F. Lu, J. Ralph and J. A. Dumesic, *Energy Environ. Sci.*, 2015, **8**, 2657–2663.
21 A. Brandt, M. J. Ray, T. Q. To, D. J. Leak, R. J. Murphy and T. Welton, *Green Chem.*, 2011, **13**, 2489–2499.
22 L. Chen, J. Dou, Q. Ma, N. Li, R. Wu, H. Bian, D. J. Yelle, T. Vuorinen, S. Fu, X. Pan and J. Y. Zhu, *Sci. Adv.*, 2017, **3**, e1701735.
23 J. Cheng, K. Hirth, Q. Ma, J. Zhu, Z. Wang and J. Y. Zhu, *Ind. Eng. Chem. Res.*, 2019, **58**, 7063–7073, DOI: 10.1021/acs.iecr.9b00931.
24 Q. Ma, J. Zhu, R. Gleisner, R. Yang and J. Zhu, *ACS Sustainable Chem. Eng.*, 2018, **6**, 14480–14489.
25 H. Bian, L. Chen, R. Gleisner, H. Dai and J. Y. Zhu, *Green Chem.*, 2017, **19**, 3370–3379.
26 Z. Wang, S. Qiu, K. Hirth, J. Cheng, J. Wen, N. Li, Y. Fang, X. Pan and J. Y. Zhu, *ACS Sustainable Chem. Eng.*, 2019, **7**, 10808–10820, DOI: 10.1021/acssuschemeng.9b01634.
27 J. Y. Zhu, L. Chen and R. Gleisner, *US Patent*, 10239905, 2019.
28 Y. Ma, Q. Xia, Y. Liu, W. Chen, S. Liu, Q. Wang, J. Li and H. Yu, *ACS Omega*, 2019, **4**, 8539–8547.
29 B. F. Ward, C. G. Force, A. M. Bills and F. E. Woodward, *J. Am. Oil Chem. Soc.*, 1975, **52**, 219–224.

30 J. Mino, E. Matijević and L. Meites, *J. Colloid Interface Sci.*, 1977, **60**, 148–153.
31 S. E. Friberg, S. B. Rananavare and D. W. Osborne, *J. Colloid Interface Sci.*, 1986, **109**, 487–492.
32 M. Hopkins Hatzopoulos, J. Eastoe, P. J. Dowding, S. E. Rogers, R. Heenan and R. Dyer, *Langmuir*, 2011, **27**, 12346–12353.
33 J. C. Del Río, J. Rencoret, P. Prinsen, A. T. Martínez, J. Ralph and A. Gutiérrez, *J. Agric. Food Chem.*, 2012, **60**, 5922–5935.
34 D. J. Yelle, J. Ralph and C. R. Frihart, *Magn. Reson. Chem.*, 2008, **46**, 508–517.
35 J. J. Stewart, T. Akiyama, C. Chapple, J. Ralph and S. D. Mansfield, *Plant Physiol.*, 2009, **150**, 621–635.
36 H. Zhou, J. Y. Xu, Y. J. Fu, H. G. Zhang, Z. W. Yuan, M. H. Qin and Z. J. Wang, *Green Chem.*, 2019, **21**, 4625–4632.
37 D. M. Miles-Barrett, A. R. Neal, C. Hand, J. R. Montgomery, I. Panovic, O. S. Ojo, C. S. Lancefield, D. B. Cordes, A. M. Slawin and T. Lebl, *Org. Biomol. Chem.*, 2016, **14**, 10023–10030.
38 S. A. Ralph, J. Ralph, L. Landucci and L. Landucci, USDA Forest Products Laboratory, Madison, WI. FPL/DFRC NMR Database -April 2009. http://www.glbrc.org/databases_and_software/nmrdatabase/NMR_DataBase_2009_Complete.pdf.
39 T. L. Lohr, Z. Li and T. J. Marks, *ACS Catal.*, 2015, **5**, 7004–7007.
40 G. Appendino, A. Minassi, N. Daddario, F. Bianchi and G. C. Tron, *Org. Lett.*, 2002, **4**, 3839–3841.
41 R. D. Offenhauser, *J. Chem. Educ.*, 1964, **41**, 39–40.
42 H. Zhou, L. Tan, Y. Fu, H. Zhang, N. Liu, M. Qin and Z. Wang, *ChemSusChem*, 2019, **12**, 1213–1221.
43 F. Xu, J. X. Sun, R. Sun, P. Fowler and M. S. Baird, *Ind. Crops Prod.*, 2006, **23**, 180–193.
44 L. Chen, J. Y. Zhu, C. Baez, P. Kitin and T. Elder, *Green Chem.*, 2016, **18**, 3835–3843.
45 R. Wang, L. Chen, J. Y. Zhu and R. Yang, *ChemNanoMat*, 2017, **3**, 328–335.
46 P. Figueiredo, C. Ferro, M. Kemell, Z. Liu, A. Kiriazis, K. Lintinen, H. F. Florindo, J. Yli-Kauhaluoma, J. Hirvonen and M. A. Kostiainen, *Nanomedicine*, 2017, **12**, 2581–2596.
47 J. Sun, C. Wang, L. P. Stubbs and C. He, *Macromol. Mater. Eng.*, 2017, **302**, 1700341.
48 S. Y. Leu and J. Y. Zhu, *BioEnergy Res.*, 2013, **6**, 405–415.
49 U. P. Agarwal, S. A. Ralph, R. S. Reiner and C. Baez, *Carbohydr. Polym.*, 2018, **190**, 262–270.
50 Y. Nishiyama, P. Langan, H. O'Neill, S. V. Pingali and S. Harton, *Cellulose*, 2014, **21**, 1015–1024.
51 P. Langan, L. Petridis, H. M. O'Neill, S. V. Pingali, M. Foston, Y. Nishiyama, R. Schulz, B. Lindner, B. Leif Hanson, S. Harton, W. T. Heller, V. Urban, B. R. Evans, S. Gnanakaran, A. J. Ragauskas, J. C. Smith and B. H. Davison, *Green Chem.*, 2014, **16**, 63–68.
52 H. Lou, J. Y. Zhu, T. Q. Lan, H. Lai and X. Qiu, *ChemSusChem*, 2013, **6**, 919–927.
53 T. Q. Lan, H. M. Lou and J. Y. Zhu, *BioEnergy Res.*, 2013, **6**, 476–485.
54 S. Nakagame, R. P. Chandra, J. F. Kadla and J. N. Saddler, *Bioresour. Technol.*, 2011, **102**, 4507–4517.
55 H. Zhu, W. Luo, P. N. Ciesielski, Z. Fang, J. Y. Zhu, G. Henriksson, M. E. Himmel and L. Hu, *Chem. Rev.*, 2016, **116**, 9305–9374.
56 J. A. Kelly, A. M. Shukaliak, C. C. Y. Cheung, K. E. Shopsowitz, W. Y. Hamad and M. J. MacLachlan, *Angew. Chem., Int. Ed.*, 2013, **52**, 8912–8916.
57 H. Bian, L. Wei, C. Lin, Q. Ma, H. Dai and J. Y. Zhu, *ACS Sustainable Chem. Eng.*, 2018, **6**, 4821–4828.
58 S. S. Nair, P. Y. Kuo, H. Chen and N. Yan, *Ind. Crops Prod.*, 2017, **100**, 208–217.
59 T. Gan, Y. Zhang, Y. Chen, H. Hu, M. Yang, Z. Huang, D. Chen and A. Huang, *Carbohydr. Polym.*, 2018, **181**, 633–641.
60 I. C. Hoeger, S. S. Nair, A. J. Ragauskas, Y. Deng, O. J. Rojas and J. Y. Zhu, *Cellulose*, 2013, **20**, 807–818.
61 E. Rojo, M. S. Peresin, W. W. Sampson, I. C. Hoeger, J. Vartiainen, J. Laine and O. J. Rojas, *Green Chem.*, 2015, **17**, 1853–1866.
62 H. Bian, L. Chen, H. Dai and J. Y. Zhu, *Carbohydr. Polym.*, 2017, **167**, 167–176.
63 N. Masruchin, B. D. Park and J. M. Lee, *Cellulose*, 2018, **25**, 7079–7090.
64 Z. Karim, M. Hakalahti, T. Tammelin and A. P. Mathew, *RSC Adv.*, 2017, **7**, 5232–5241.
65 K. L. Spence, R. A. Venditti, O. J. Rojas, Y. Habibi and J. J. Pawlak, *Cellulose*, 2010, **17**, 835–848.
66 I. Solala, A. Volperts, A. Andersone, T. Dizhbite, N. Mironova-Ulmane, A. Vehniäinen, J. Pere and T. Vuorinen, *Holzforschung*, 2012, **66**, 477–483.
67 E. S. Kim, S. Liu, M. M. Abu-Omar and N. S. Mosier, *Energy Fuels*, 2012, **26**, 1298–1304.
68 Y. Lu and N. S. Mosier, *Biotechnol. Bioeng.*, 2008, **101**, 1170–1181.
69 R. Weingarten, J. Cho, W. C. Conner Jr. and G. W. Huber, *Green Chem.*, 2010, **12**, 1423–1429.
70 H. Ji, J. Y. Zhu and R. Gleisner, *RSC Adv.*, 2017, **7**, 46208–46214.
71 X. Luo, R. Gleisner, S. Tian, J. Negron, W. Zhu, E. Horn, X. Pan and J. Zhu, *Ind. Eng. Chem. Res.*, 2010, **49**, 8258–8266.
72 H. Zhou, J. Y. Zhu, X. Luo, S.-Y. Leu, X. Wu, R. Gleisner, B. S. Dien, R. E. Hector, D. Yang, X. Qiu, E. Horn and J. Negron, *Ind. Eng. Chem. Res.*, 2013, **52**, 16057–16065.
73 J. Zhu, L. Chen, R. Gleisner and J. Y. Zhu, *Fuel*, 2019, **254**, 115572, DOI: 10.1016/j.fuel.2019.05.155.
74 H. Ji, L. Chen, J. Zhu, R. Gleisner and X. Zhang, *Ind. Eng. Chem. Res.*, 2016, **55**, 11253–11259.
75 K. Lundquist, R. Simonson and K. Tingsvik, *Sven. Papperstidn.*, 1980, **83**, 452–454.
76 X. Yang, N. Li, X. Lin, X. Pan and Y. Zhou, *J. Agric. Food Chem.*, 2016, **64**, 8379–8387.